Improvement of AEP Predictions Using Diurnal CFD Modelling with Site-Specific Stability Weightings Provided from Mesoscale Simulation

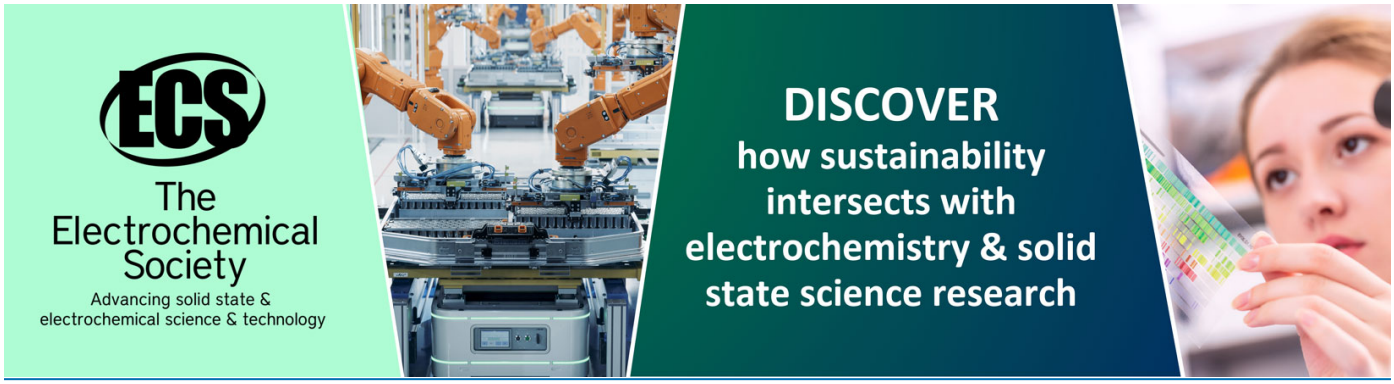

Improvement of AEP Predictions Using Diurnal CFD Modelling with Site-Specific Stability Weightings Provided from Mesoscale Simulation

Y Hristov, G Oxley and M Žagar

Vestas Wind Systems A/S, Hedeager 42, Aarhus North, Denmark, 8200

Email: yavhr@vestas.com

Abstract. The Bolund measurement campaign, performed by Danish Technical University (DTU) Wind Energy Department (also known as RISØ), provided significant insight into wind flow modeling over complex terrain. In the blind comparison study several modelling solutions were submitted with the vast majority being steady-state Computational Fluid Dynamics (CFD) approaches with two equation k-ε turbulence closure. This approach yielded the most accurate results, and was identified as the state-of-the-art tool for wind turbine generator (WTG) micro-siting. Based on the findings from Bolund, further comparison between CFD and field measurement data has been deemed essential in order to improve simulation accuracy for turbine load and long-term Annual Energy Production (AEP) estimations. Vestas Wind Systems A/S is a major WTG original equipment manufacturer (OEM) with an installed base of over 60GW in over 70 countries accounting for 19% of the global installed base. The Vestas Data Centre (VDC) provides online live data to more than 47GW of these turbines allowing a comprehensive comparison between modelled and real-world energy production data. In previous studies, multiple sites have been simulated with a steady neutral CFD formulation for the atmospheric surface layer (ASL), and wind resource (RSF) files have been generated as a base for long-term AEP predictions showing significant improvement over predictions performed with the industry standard linear WAsP tool. In this study, further improvements to the wind resource file generation with CFD are examined using an unsteady diurnal cycle approach with a full atmospheric boundary layer (ABL) formulation, with the unique stratifications throughout the cycle weighted according to mesoscale simulated sectorwise stability frequencies.

1. Introduction

AEP estimation for a wind farm is a vital step in the planning phase of new wind farm projects. The size of wind farms has increased significantly from landowners with 1-5 WTGs, to massive energy sector developers using wind as an investment base with projects usually consisting of at least 100 WTGs. Taking into account the average price per MW installed capacity in 2011 wind investments are now in the hundreds of millions Euros, according to the Bloomberg New Energy Finance's Wind Turbine Price Index [1]. Hence, the financial consortiums securing the funding of these projects have a very high demand for increased business case certainty. In addition, lowering the levelized cost of energy (LCOE) is a very important factor for wind farm developers to maximize their profit margins. Since many of the best wind resources available on relatively non-complex terrain sites have already been exploited, many developments are exploring mountainous areas with consistently complex

terrain. The obvious advantage is the higher wind speeds due to the speed-up effects, but increases in turbulence and rapid wind direction changes are commonly present as well.

The traditional tools for siting flow field calculations have been based for many years on linear flow models, such as WAsP [2] developed by the DTU Wind Energy Department. Refinements and improvements of the process behind the WAsP tool have been made through its 25 years of existence in order to improve speed, robustness and precision [3]. Although very efficient in comparison to the non-linear CFD approaches, it is well known that linear flow models cannot resolve flow detachment and recirculation, which become increasingly important in complex terrain analysis and evident in the Bolund blind comparison results [4]. The WAsP tool gives good results in areas with less than 18° terrain slope, or approximately 30%, but can also be used on more complex sites knowing well the limitations of the linear flow model. Considering the above, DTU Wind Energy Department has announced the introduction of a new WAsP CFD tool for wind resource assessment in complex terrain based on the EllipSys code [5], their in-house finite volume CFD solver developed since the mid-1990s.

CFD is integral part of the Vestas micro-siting activities. Large amount of site have been analysed, giving us a wide range of experience in CFD's application to turbine micro-siting, specifically in obtaining engineering quantities of interest, including turbulence intensity, wind shear, wind veer and flow inclination. The model results were also compared to the publicly available datasets of Bolund [4], and Askervein [6] field measurement campaigns. Overall, these validation studies give very good confidence in the model performance.

CFD in Vestas has been also used as a base for wind resource file generation for AEP predictions [7]. A benchmarking project was undertaken, in which a statistically significant number of sites of varying complexity were analysed comparing actual production values with the a priori CFD and WAsP (No ΔRIX correction applied) AEP calculations. Figure 1 demonstrates the AEP percentage improvement in the CFD vs. WAsP predictions across the 50 sites analysed. Overall, it was determined that by using a neutral CFD model of the atmospheric surface layer (ASL), we can expect a roughly 8% improvement in the mean error.

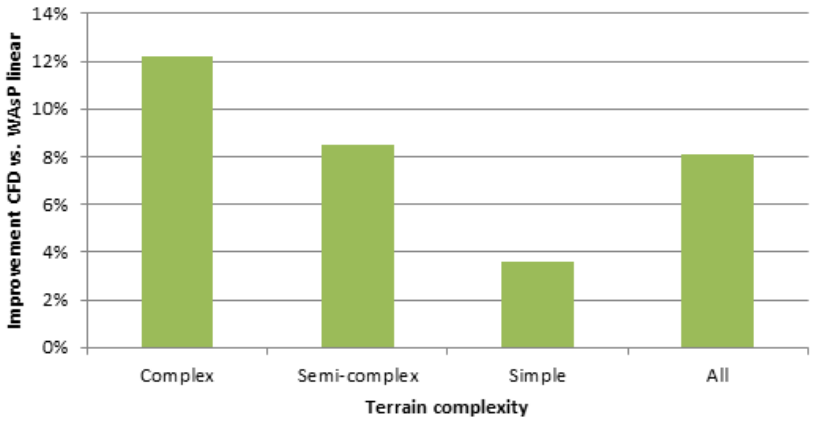

Figure 1. AEP percentage improvement for 50 sites using neutral CFD vs. linear WAsP model

However, the limitations of the CFD ASL model are well known, and in order to increase AEP prediction accuracy, it is necessary to increase the complexity of the flow physics considered. In this paper, the flow model is extended to include the important variability in stability stratifications on site and allow for this variability in the overall AEP predictions.

2. Maximum Mixing Length – Limited *k-ε* CFD ABL model

Traditionally, CFD micro-scale modelling for loads and AEP predictions has been limited to the ASL using steady-state isothermal CFD approaches with two-equation turbulence closure (*k-ε* and *k-ω*). In order to improve on these predictions, it is necessary to shift towards a model suitable for the entire atmospheric boundary layer (ABL) through the inclusion of the important Coriolis and buoyancy forces and consideration of heat transfer processes which have been mostly neglected to date. In this work, a maximum mixing length-limited *k-ε* CFD ABL model is used. In the standard *k-ε* formulation applied to ABL flows, the flow is too diffusive due to a monotonically increasing turbulent mixing length. In this maximum mixing length-limited formulation, the turbulent mixing length is capped. Detailed formulation of the method can be found in Sogachev et al [8] and Koblitz [9], while important details of the formulation are included here for clarity.

2.1. Formulation

The transport equations for turbulent kinetic energy, *k*, and turbulent diffusion rate, *ε*, are:

$$\frac{\partial k}{\partial t} + U_i \frac{\partial k}{\partial x_i} - \frac{\partial}{\partial x_i}\left(\frac{\nu_t}{\sigma_k}\frac{\partial k}{\partial x_i}\right) = P_k - \varepsilon + B \tag{1}$$

$$\frac{\partial \varepsilon}{\partial t} + U_i \frac{\partial \varepsilon}{\partial x_i} - \frac{\partial}{\partial x_i}\left(\frac{\nu_t}{\sigma_\varepsilon}\frac{\partial \varepsilon}{\partial x_i}\right) = \frac{\varepsilon}{k}(C_{\varepsilon 1}^{*} P_k - C_{\varepsilon 2}\epsilon + C_{\varepsilon 3} B) + D \tag{2}$$

P_k represents the shear production while B is the buoyant production term given by:

$$B = \frac{\beta \nu_t}{Pr_t}\vec{g} \cdot \nabla\theta \tag{3}$$

Where β is the coefficient of thermal expansion of air, ν_t is the turbulent kinematic viscosity, Pr_t is the turbulent Prandtl number, $\vec{g}$ is the gravitational acceleration and θ is the potential temperature. Turbulence coefficients are selected as proposed by Sogachev et al [8] and shown in Table 1.

Table 1. Maximum mixing length-limited *k-ε* coefficients

C_μ	$C_{\varepsilon 1}$	$C_{\varepsilon 2}$	$C_{\varepsilon 3}$	σ_k	σ_ε	Pr_t
0.03	1.52	1.83	Eqn.(8)	2.95	2.95	Eqn.(11)

The modified $C_{\varepsilon 1}^{*}$ constant is given by:

$$C_{\varepsilon 1}^{*} = C_{\varepsilon 1} + (C_{\varepsilon 2} - C_{\varepsilon 1})\frac{l_t}{l_e} \tag{4}$$

which is dependent on the ratio of local turbulent mixing length, l_t, to the maximum mixing length, l_e, for the flow. When this ratio is unity, $C_{\varepsilon 1}^{*} = C_{\varepsilon 2}$, so that the production and dissipation terms in the diffusion transport equation are balanced. When $l_t << l_e$, $C_{\varepsilon 1}^{*} = C_{\varepsilon 1}$ and the modified term still satisfies the logarithmic velocity profile in the ASL. The turbulent mixing length is given by:

$$l_t = C_\mu^{3/4} \frac{k^{3/2}}{\varepsilon} \tag{5}$$

In this work the Mellor-Yamada formulation [10] is chosen for the maximum mixing length, l_e, because of its suitability in dealing with variable ABL heights associated with general thermal stratifications of the atmosphere.

$$l_e = \alpha \frac{\int_0^\infty z\sqrt{k}dz}{\int_0^\infty \sqrt{k}dz} \tag{6}$$

Where $\alpha=0.075$ is used to ensure the proper maximum mixing length is returned in neutral conditions. An additional source term, D, is found in the dissipation equation (2). Numerical experiments have shown some differences in the behavior of the k-ε and k-ω turbulence models, with the k-ω model performing slightly better specifically in canopy flows. As proposed by Sogachev et al, this source term, equation (7), is added to allow the k-ε formulation to behave similarly to the k-ω formulation and is included in this work because of its eventual extension to canopy flows.

$$D = C_\mu \left[\left(\frac{1}{\sigma_k} - \frac{1}{\sigma_\varepsilon} \right) k \frac{\partial^2 k}{\partial x_i^2} - \left(\frac{1}{\sigma_k} + \frac{1}{\sigma_\varepsilon} \right) \frac{k}{\varepsilon} \frac{\partial \varepsilon}{\partial x_i} \frac{\partial k}{\partial x_i} + \frac{2}{\sigma_k} \frac{\partial k}{x_i} \frac{\partial k}{x_i} \right] \tag{7}$$

As opposed to other models, the $C_{\varepsilon 3}$ coefficient is not defined a priori, but is calculated locally according to a stability-related coefficient α_B:

$$C_{\varepsilon 3} = (C_{\varepsilon 1} - C_{\varepsilon 2})\alpha_B + 1 \tag{8}$$

where

$$\alpha_B = \begin{cases} 1 - \dfrac{l_t}{l_e} & for\ Ri_g > 0 \\ 1 - \left[1 + \dfrac{C_{\varepsilon 2} - 1}{C_{\varepsilon 2} - C_{\varepsilon 1}} \right] \dfrac{l_t}{l_e} & for\ Ri_g < 0 \end{cases} \tag{9}$$

Ri_g is defined as the local gradient Richardson number

$$Ri_g = \frac{B}{P_k} \tag{10}$$

In addition the turbulent Prandtl number, Pr_t, is calculated according to:

$$Pr_t = \begin{cases} 0.74 & for\ Ri_g < 0 \\ 0.74\left(1 - 15Ri_g\right)^{-1/4} & for\ Ri_g > 0 \end{cases} \tag{11}$$

3. Wind Resource (RSF) File Generation

3.1. Mesoscale/CFD simulation and stability weightings

It is not common for the meteorological masts set up by wind power developers to be equipped with the necessary instrumentation required to sample atmospheric stability, such as differential temperature measurements. As an alternative a mesoscale model can be used to determine the frequency of different stability conditions occurring within each of the 36 directional sectors, in addition to typical diurnal surface temperature variations. These are then used as input to the CFD simulation.

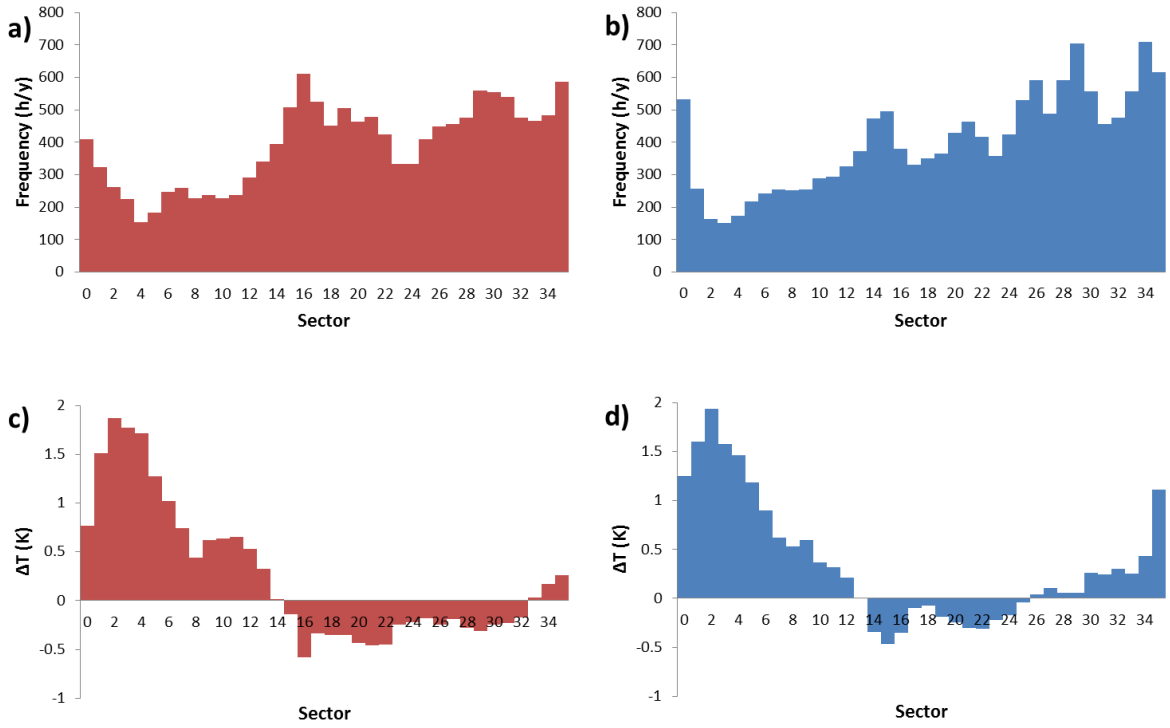

Figure 2: A comparison between measured (red colour, a, c) and WRF-ARW simulated (blue colour, b, d) wind direction frequency (top row, a, b) and average vertical temperature difference between 80 m and 10 m above surface (bottom row, c, d) for 2 years of data from a meteorological mast in flat terrain at mid-latitude.

Meteorological input for the CFD modelling process is obtained by running the WRF-ARW model [11] forced with the GFS final analyses for a period of 14 years, to create mesoscale climatology with 3 km horizontal resolution. For a point of interest, the representative free atmosphere wind, atmospheric stability conditions, and diurnal surface temperature evolution are extracted. By not using the horizontal pressure gradient to define the geostrophic wind we allow for ageostrophic wind components, for example caused by large scale terrain channelling, which can sometimes represent a significant part of the available wind energy. Low level jets, however, are generated in the diurnal CFD simulation, as described in the following section. Stability is defined as a vertical temperature gradient across a rotor plane. An example of a comparison between observed temperature gradient (as already mentioned above, good measurements of this variable are extremely rare on wind energy development sites) and its simulated counterpart is shown in Figure 2. Our experience with using the mesoscale model for qualitative and quantitative description of atmospheric stability effects on local wind conditions has been quite positive.

The process of RSF generation from the mesoscale input through CFD simulations to final weighting of various flow solutions can be outlined as follows:

a. Mesoscale simulation to obtain site-specific stability rose, geostrophic conditions and typical diurnal surface temperature cycles.

b. 1D CFD simulation to obtain time dependent diurnal profiles of velocity, potential temperature, turbulent kinetic energy and turbulent dissipation rate using results of the mesoscale simulation in a).

c. Full CFD simulation using mapped 1D simulation profiles as dynamic inlets, while still imposing the same uniform surface temperature cycle. Data is dumped at 2hr intervals containing hub-height isosurfaces of wind speed and met mast wind shear.

d. Individual met mast shear and hub-height wind speed isosurfaces are weighted and combined according the mesoscale determined frequency of that particular stability class. These are then used as input to the RSF procedure below.

3.2. RSF procedure

The wind resource file generation (RSF) process uses the calculated wind speeds from the 36 sector CFD simulations as well as multiple met mast data long term corrected to Vestas 14 year mesoscale WRF model predictions. The steps in RSF file generation are:

a. Flow simulation (CFD ABL model)

b. Long-term correction (LTC) using sectorwise linear regression of met mast wind speed data with 14 year mesoscale data [12]

c. Extrapolate met mast wind speed to hub height according to the CFD ABL model predicted wind shear between mast measurement height and hub height.

d. 3D inverse distance interpolations for extrapolated met mast wind speeds and wind direction frequencies to give S_{mast_map} and f_{map}. Suppose we have observations $u(x_i)$ for three dimensional points x_i for $i = 0,1,2,...,N$, then the interpolation at point p is $u(p)$

$$u(p) = \frac{\sum_{i=0}^{N} w_i(p) u(x_i)}{\sum_{j=0}^{N} w_j(p)} \tag{12}$$

Where

$$w_i(p) = \frac{1}{d(p, x_i)^2} \tag{13}$$

for some distance function $d(x, y)$. Here, the Euclidean distance function is used with the exception that the vertical dimension is scaled according to the aspect ratio between the horizontal and vertical planes.

e. Calculate scaling factors for CFD ABL model wind velocity field to match wind speed measurements at the mast positions giving a scaled wind speed map:

$S_{mast\_map} \rightarrow S_{scaledCFD\_map}$. These scaled sectorwise CFD wind speed maps are then combined according to:

$$\bar{S}_{scaledCFD\_map} = \frac{1}{s}\sum_{sec} f_{map} S_{scaledCFD\_map} \quad (14)$$

f. Finally, the RSF file is created for 25m horizontal resolution with directional wind distribution and frequencies being used to calculate the Weibull parameters for each mesh point in the wind resource domain

3.3. Turbine production data

Production data is obtained from the Vestas Data Centre, which collects data 24/7 from all connected Vestas turbines. The AEP is calculated from the filtered data and normalized to average year AEP. In the original benchmarking study, a statistically significant number of wind farms in operation for more than 2 years in the period 2000-2013 and more than 95 % data recovery rate were used.

4. Results

For this initial study into the viability of diurnal CFD simulation for AEP estimations, a site was selected from the original 50 site benchmark for which both WAsP and the CFD ASL model had difficulty predicting AEP. Figure 3 illustrates the test site chosen, with fairly benign topography as well as a dominant wind direction from the south-west quadrant. When using WAsP and CFD ASL model, AEP prediction errors of 16% and 14% are found respectively, leaving a large amount of room for improvement for the predictions performed with the CFD ABL model.

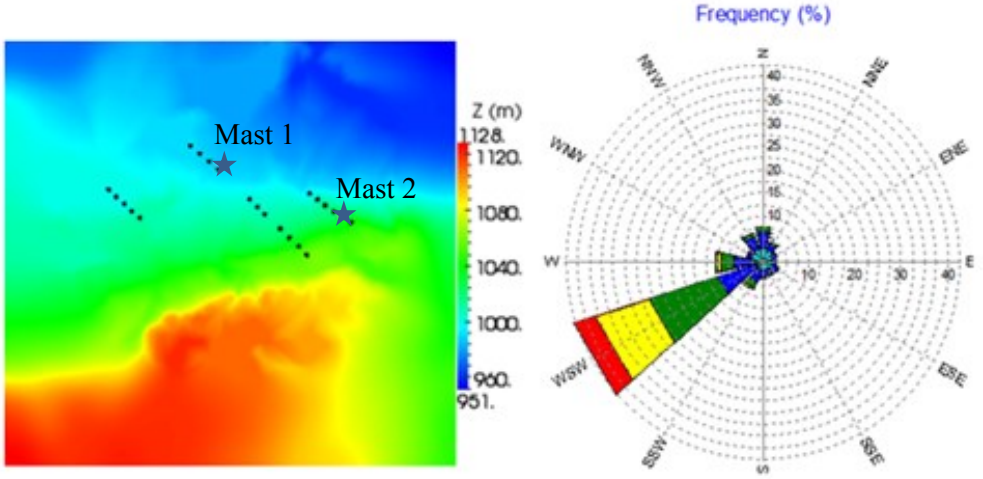

Figure 3. Topography, turbine (dots) and mast (star) layout (left) and wind frequency distribution (right) for the selected test site.

Figure 4 demonstrates the results of the mesoscale simulation using WRF-ARW version 3.3.1[11] coupled into the GFS final analyses providing global 3km resolution mesoscale climatology with very high vertical resolution in the lower boundary layer to accurately capture relevant atmospheric features. Here, the stability rose is shown for various stability classes, as well as a typical site-specific diurnal surface temperature cycle for a representative day.

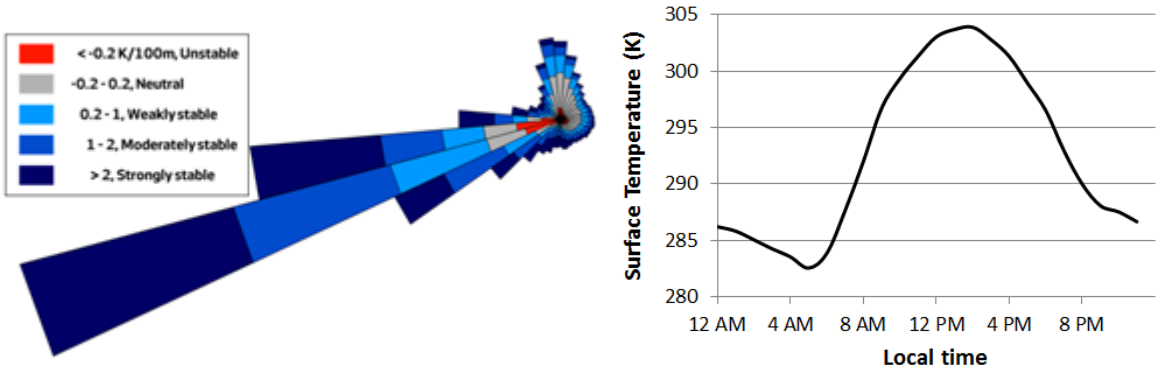

Figure 4. Mesoscale simulation results at a representative grid point including the stability rose (left, expressed as vertical gradient of potential temperature) and diurnal surface temperature cycle for a typical day (right).

Using this information, the diurnal simulations were clustered around the 230, 240 and 250 wind sectors with the surface temperature cycle in Figure 4 imposed on both the 1D and full CFD simulations. Figure 5 demonstrates the time evolution of the vertical profiles of horizontal velocity and potential temperature. It is found that typically 4-5 cycles are required to obtain periodic results. It is at this point that the profiles are used as input to the full simulation.

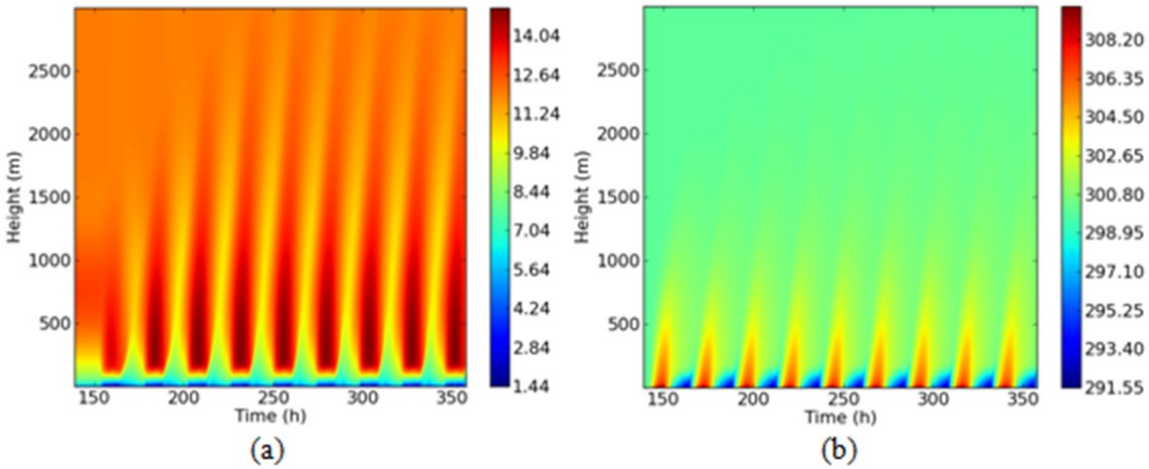

Figure 5. 1D precursor simulation profiles (a) horizontal velocity (m/s) and (b) potential temperature (K). Note: the horizontal axis scale begins at 150hr as the 1D precursor requires this amount of time to be run in purely neutral conditions in order for the flow to reach a balance with the geostrophic and Coriolis forcing.

Figure 6 demonstrates the time history of turbulence intensity and wind shear through the full simulation with the expected trends. Stable flow periods are characterized by a positive potential temperature gradient, low turbulence intensity and high shear, which non-stable flow periods are characterized by negative temperature gradient, higher turbulence intensity and very low shear. The unphysical spike in wind shear is noted and will be further investigated. For this study this range was omitted from the weighting.

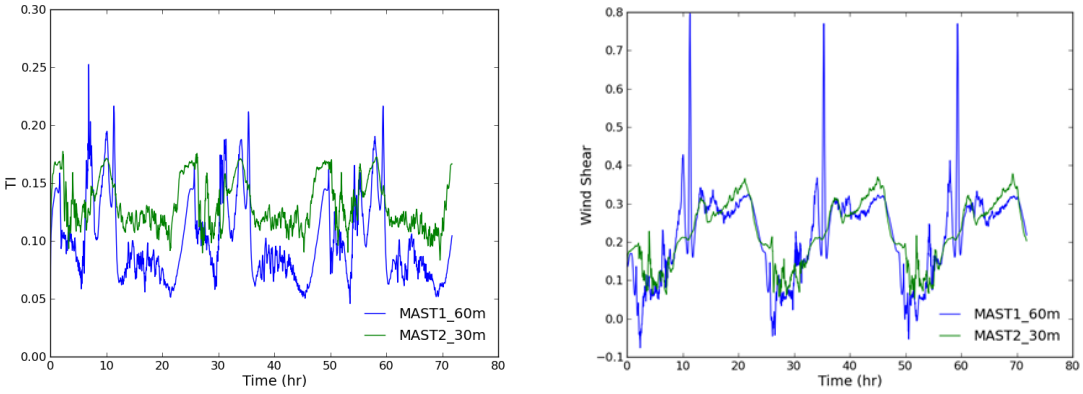

(a) (b)

Figure 6. Time history of met mast (a) turbulence intensity and (b) wind shear based on 10 min. averaging window. Results shown are for sector 250.

The stability frequency rose in Figure 4 suggests it is appropriate to use the weightings listed in Table 2 when averaging the individual results available at 2hr intervals for each sector of interest. In this context, the weighting is applied to all results obtained through the cycle.

Table 2. Test site sectorwise stability weightings

	Sector 230	Sector 240	Sector 250
Stable	25%	39%	54%
Neutral/Unstable	75%	61%	46%

Using the above weightings, the AEP estimation using the CFD ABL model is calculated and compared to the actual, WAsP predicted and CFD ASL model predicted AEPs. AEP predictions with WAsP, CFD ABL and ASL models are done using the same LTC data set.

Table 3. Comparison of test site AEP predictions with various flow models

Actual	WAsP	CFD ASL	CFD ABL
200.2	231.6	228.2	207.0
Error	16%	14%	3%
			(GWh/yr)

5. Discussion

It is found in this initial study, that using a diurnal cycle in a CFD ABL model has significantly lowered the AEP estimation error for this particular test site to 3% of the actual production value. The weighted average of the met mast shear and hub height wind speed isosurfaces give a more physical representation of actual on-site conditions. These results warrant further investigation into the approach to, as with the CFD ASL model, perform a statistically significant number of AEP estimations for sites of varying complexity in order to further prove the usefulness of the method and get a better definition of the uncertainties involved. In addition, similar comparison with the WAsP CFD model instead of the WAsP linear model is planned.

References

[1] Feinberg S Wind turbine prices fall to lowest in years http://bnef.com/PressReleases/view/139 Publication Date: 07 Feb 2011.
[2] WAsP – the Wind Atlas Analysis and Application Program; www.wasp.dk
[3] Petersen E L, Mortensen N G, Landberg L, Højstrup J and Frank H P 1998 Wind Power

Meteorology Part I: Climate and turbulence. *Wind Energy* **1** 2-22.
[4] Bechmann A, Sørensen N N, Berg J, Mann J, Réthoré P E 2011 The Bolund Experiment, Part II: Blind comparison of microscale flow models. *Boundary-Layer Meteorol.* **141** 245–271.
[5] EllipSys 2D/3D. Wind Energy Department, DTU, Denmark http://www.risoe.dtu.dk/research/sustainable_energy/wind_energy/projects/numwind/ellipsys.aspx?sc_lang=en
[6] Taylor P, Teunissen H 1984 The Askervein Hill project: report on the Sept./Oct. 1983, main field experiment *Ontario Technical Report MSRB-84-6. Atmospheric Environment Service*
[7] Mogensen S H, Hristov Y V, Knudsen S J, Oxley G 2012 Validation of CFD wind resource mapping in complex terrain based on WTG performance data *EWEA 2012 Conference Proceedings*
[8] Sogachev A, Kelly M and Leclerc M Y 2012 Consistent two-equation closure modelling for atmospheric research: buoyancy and vegetation *Boundary-Layer Meteorol.* **145** 307-327
[9] Koblitz T 2013 CFD simulation of non-neutral atmospheric boundary layer conditions *PhD thesis - DTU Institute for Wind Energy*
[10] Mellor G L and Yamada T 1974 A hierarchy of turbulence closure models for planetary boundary layers *J Atmos Sci*. **31** 1791–1806
[11] Skamarock W C, Klemp J B, Dudhia J, Gill D O, Barker D M, Duda M G, Huang X Y, Wang W, and Powers J G 2008 A description of the Advanced Research WRF version 3. *NCAR Technical Note NCAR/TN475 + STR.* http://www.mmm.ucar.edu/wrf/users/docs/arw_v3.pdf
[12] Thoegersen M L, Motta M, Soerensen T, Nielsen P 2007 Measure-Correlate-Predict Methods: Case Studies and Software Implementation, *EWEC 2007 Proceedings*